A data-driven approach for scour detection around monopile-supported offshore wind turbines using Naive Bayes Classification

Satish Jawalageri[a,b*], Ramin Ghiasi[a], Soroosh Jalilvand[b], Luke J. Prendergast[c], Abdollah Malekjafarian[a]

[a] Structural Dynamics and Assessment Laboratory, School of Civil Engineering, University College Dublin, Dublin, Ireland.
[b] Gavin and Doherty Geosolutions, Dublin, Ireland.
[c] Department of Civil Engineering, Faculty of Engineering, University of Nottingham, Nottingham, NG7 2RD, United Kingdom

***** Corresponding author, Email address: satish.jawalageri@ucdconnect.ie

Abstract

This paper proposes a novel data-driven framework for scour detection around offshore wind turbines (OWTs), where damage features are derived from wind and wave-induced acceleration signals collected along the tower. A numerical model of the NREL 5 MW wind turbine, which considers aerodynamic and hydrodynamic loading with soil-structure interaction (SSI) and servo-dynamics, is developed. The model is used to simulate the acceleration responses along the tower for a healthy structure, and a structure affected by progressive scour. A data segmentation process is initially performed on the collected data, which is followed by a feature selection scheme based on the analysis-of-variance (ANOVA) algorithm, to eliminate irrelevant characteristics from the time domain feature set of responses. The proposed framework consists of two main components: (a) offline training, and (b) real-time classification. The acceleration responses collected from the healthy structure and the structure subjected to three different damage scenarios (different scour depths) and under various load conditions, are used in the offline training mode. The selected feature vector from the feature extraction process is used as input to a Naive Bayes classifier (NBC) algorithm to train the model. In the real-time classification, a prediction of the scour depth affecting the structure is performed using a new dataset simulated from unseen load cases and scour conditions of the OWT. The results show that the model trained in the offline stage can predict the scour depth in the real-time monitoring stage with performance measures over approximately 94%.

Keywords: Offshore wind turbines, Monopile, Scour, Feature extraction, Naive Bayes, Real-time prediction.

1. Introduction

Offshore wind turbines (OWTs) have been rapidly deployed in Europe over the last few years. 236 GW of wind power capacity is installed across Europe of which 28 GW is from offshore turbines as of 2021 (WindEurope 2021). European Governments aim to achieve 160 GW of installed offshore wind capacity by 2030 (WindEurope 2022). This ambition of achieving larger capacity in such a short time will require advances in wind turbine generator (WTG) technologies, which will eventually be achieved by the use of larger turbine sizes. Recently, the World's largest offshore wind turbine, a 14 MW prototype by Siemens Gamesa, has been developed, demonstrating the upward trajectory. Furthermore, there are plans for the installation of these larger turbines at Moray West project in Scotland (Biogradlija 2022), which further shows how rapidly the technology is advancing. As turbine sizes increase to generate more power, the loads experienced by the turbine also increase. This is because larger wind turbines have longer blades to harness more wind energy, resulting in higher loads

acting on the blades and the nacelle. To support the increased size and weight of larger wind turbines, larger foundations are required, which results in higher loads applied to the substructure. This can potentially lead to an increased probability of damage occurrence in the main structure and its substructures.

Over 80% of OWTs installed to date have been supported by monopile foundations driven into the seabed, with jacket foundations representing approximately 15% of support structures (WindEurope 2021). Monopiles are a well-known and reliable foundation solution in the offshore wind industry with an extensive track record of successful installation. To date, monopile foundations have typically been installed in average water depths of around 30 m (Wang et al. 2018). However, advances in technology and the development of a new generation of super-large (XXL) monopiles have made it possible to install monopiles in deeper water depths up to 60 m. These XXL monopiles have diameters of circa. 8 m to 10 m (Shadlou and Bhattacharya 2016). In addition to water depths, the strength of the soil and loads acting on the structure are significant factors that drive the design of monopile foundations. The soil strength and stiffness can vary widely from site to site, and monopile designs must be able to account for these variations to ensure that the foundation can withstand the forces exerted by environmental wind and wave loads. Monopile design requires careful consideration of the pile head rotation and displacement to ensure it remains within the permissible limits defined under the Ultimate and Serviceability Limit States (DNVGL 2016); Sánchez et al. (2019).

In general, OWTs are exposed to harsh environmental conditions that can gradually weaken their structural integrity over time, resulting in reduced efficiency and effectiveness, which may lead to structural damage occurrence. Factors such as environmental exposure, fatigue, soil strength deterioration, poor construction, and maintenance practices, can all contribute to this degradation. Structural Health Monitoring (SHM) approaches can play a vital role in detecting this damage in the early stage, which can potentially result in avoiding catastrophic failure of OWT structures (Tian et al. 2020).

Failure of OWT structures may be caused by many damaging phenomena such as corrosion, boat collision, and high storm loading, among other causes. (Kolios et al. 2018). However, one of the main causes of failure is due to the occurrence of scour erosion around the foundation, which removes soil material due to the action of currents, tides, and waves. Monopiles are highly sensitive to scour occurrence, which reduces the strength and stiffness of these foundations (Peder Hyldal Sørensen and Bo Ibsen (2013), Prendergast et al. (2015)). There have been many studies focussed on the use of SHM techniques for monopile scour detection such as acoustic emission monitoring, thermal imaging method, Ultrasonic Testing (UT) methods, fatigue and modal property monitoring, and strain monitoring, among others (Weinert et al. (2015), Kolios et al. (2018), Devriendt et al. (2014), Civera and Surace (2022)). Currently, most maintenance companies use bathymetric data to detect the presence of scour holes (Kolios et al. 2018). However, these measurements cannot quantify the impact of the presence of a scour hole on the dynamic behaviour of a structure and its fatigue life (Weijtjens et al. 2016). Furthermore, it is difficult to predict the extent of scour around a given foundation as this tends to constantly evolve due to seabed currents and wave actions during operational conditions (Whitehouse et al. 2008). In addition, various measurement techniques have been employed currently at intervals ranging from six months to five years to assess scour, a critical concern in OWT projects. These techniques include sidescan sonar, which is deployed from vessels to capture seabed images; multibeam sonar, also vessel-based, for mapping the seafloor; remotely operated vehicles (ROVs) equipped with specialized tools for seabed inspections; and finally, visual inspections or video recordings (Duguid 2017). These methods collectively enable the monitoring and evaluation of seabed conditions, helping to detect and address potential issues such as sediment erosion around the foundation of OWTs.

Scour erosion around monopile foundations has an influence on the dynamic properties of the structure such as natural frequencies and mode shapes, and its occurrence might eventually lead to resonance in the structure from an interaction of the damaged natural frequencies and environmental and rotor frequencies (Tempel et al. 2004). There are many studies which investigate the influence of the presence of scour around monopile structures on the natural frequencies, mode shapes, and system deflections (Reese et al. (1989), Bennett et al. (2009), Nanda Kishore et al. (2009), Achmus et al. (2010), Prendergast et al. (2015), Jawalageri et al. (2022)). The most common conclusion is that scour leads to a reduction in the system natural frequencies, increasing risk of resonance with the rotor (1P) frequency, and the wave spectrum for large structures.

Sensors installed along OWTs can be used to obtain data that can subsequently be used to investigate the presence of scour, and obtain the natural frequencies and mode shapes of OWT structures. There are many sensors that can potentially be used for scour damage detection such as accelerometers, displacement sensors, inclinometers, and others. Accelerometers tend to be the most common, and can be used to collect the acceleration responses of the system, which can be used for fatigue analysis, damage detection, and modal identification (Kolios et al. 2018). Tang and Zhao (2021) investigated a numerical model and monitoring system for a monopile-supported wind turbine to evaluate the impact of scour erosion on its structural integrity. The study proposes two early-warning indicators based on dynamic characteristics informed from accelerometers, and dynamic response analyses informed from inclinometers, which can reflect the basic characteristics of how scour affects the structure, and can be used simultaneously for mutual verification of safety judgements. Mayall et al. (2018) conducted experiments on a 1:20 scale OWT model with accelerometers, force sensors, strain gauges and displacement sensors installed along the structure to investigate changes in the dynamic response under the presence of scour erosion and scour protection. Results suggest that the second and third vibration modes are more sensitive to scour, and sediment deposited within the scour protection material could lead to an increase in the natural frequency of the structure. Prendergast et al. (2015) investigated the effect of scour on the natural frequencies of a scale-model monopile with installed accelerometers, in order to validate a numerical model of a full-scale OWT supported on a monopile foundation. The results showed that the natural frequency of the full-scale system decreased with increasing scour depth, and the changes in frequency were relatively larger for the structure installed in loose sand than in dense sand. Jawalageri et al. (2022) used simulated acceleration data to detect the change in natural frequencies and mode shapes of a 5 MW OWT under various local scour conditions around a monopile foundation. They conclude that the second mode shape exhibits more sensitivity to scour than the first mode shape. Michalis et al. (2013) presented a scour monitoring system consisting of small capacitive scour probes installed around a foundation structure of an OWT. These were linked to a wireless network for remote data acquisition. The sensor was evaluated through laboratory experiments simulating different underwater conditions, and the results indicated that it can monitor seabed degradation, scour, and sediment deposition processes.

Many of the previous approaches rely on the creation of a reference finite-element model or manual interpretation of measured data for the purpose of scour detection, which is a drawback as models may not match the real conditions. As an improvement, data-driven algorithms and machine learning (ML)-based methods have been extensively employed in recent years to detect damage in OWTs using data extracted from vibration sensors. Jeong et al. (2020) proposed a novel method on data fusion of acceleration and angular velocity responses to detect damage occurrence near the bottom of a monopile. They developed a damage index using power spectral density from accelerometers and a gyroscope. The results showed that natural frequency of the monopile decreased with an increase in damage severity due to scour. Zhang et al. (2018) proposed a support vector machine (SVM)-based approach using acceleration data for SHM of OWTs. They developed online time-domain and

frequency-domain SVM classifiers using the data collected from a real OWT. They showed that time domain SVM can classify the abnormal conditions. Mousavi et al. (2020) investigated the vibration signals of an offshore jacket structure where the frequencies were obtained from frequency domain decomposition (FDD). These frequency data were used to train a deep neural network (DNN). They showed that the proposed DNN method can predict the damage in the presence of uncertainties. Schröder et al. (2017) employed a two-step algorithm to detect the damage in OWTs using sequential quadratic programming method. Different measures based on eigenfrequencies, mode shapes, and time series data are employed for damage localization, and the effectiveness of the algorithm is demonstrated through numerical models and lab-scaled structures with simulated and real damage, respectively.

The above research demonstrates that data-driven methods for damage detection in OWTs are gaining traction. However, few studies exist that focus on the use of data-driven algorithms for the detection of scour around OWTs. In this paper, a novel data-driven algorithm is developed whereby it is assumed that the acceleration data measured at several points along an OWT tower are available for damage detection. The proposed algorithm is composed of three main components: In the first component, a feature selection scheme based on the analysis-of-variance (ANOVA) (Kim 2017) algorithm is used to reduce the dimensionality of the original data by eliminating irrelevant characteristics from the set of time domain features extracted from the signals. Furthermore, it minimizes intraclass distances and maximizes distances between damage classes. Then, selected feature vector will serve as input to a Naive Bayes Classifier (NBC) (Soria et al. 2011) algorithm as the second component. An offline training strategy is used to reach a well-trained ML algorithm. Finally, a real-time prediction of the scour depth of the structure is developed using the proposed framework by providing a new sample associated with unseen load cases or scour depths of the OWT. The NREL 5 MW (Jonkman et al. 2009) OWT is modelled using OpenFAST and SESAM software. The model is used to simulate acceleration responses in the structure, which are used for validation of the proposed methodology. The simulations are performed with the presence of different scour depths and different operational conditions for the case of an OWT installed in medium dense sand.

The primary focus of this research is on scour as a form of damage, and the proposed approach is tailored specifically for detecting scour-induced changes in dynamic properties. However, the study acknowledges that other types of damage, such as cracks or corrosion, can also lead to changes in the dynamic properties of structures. While the current research is focused on scour, it is indeed possible to extend the same approach to identify and assess these other forms of damage. By adapting the methodology and incorporating the relevant features associated with different types of damage, the approach could be applied to provide a broader assessment of structural health, covering a range of potential damage scenarios beyond scour.

2. Numerical modelling

Numerical modelling of OWTs has been challenging in the literature as structures are under a complicated set of wind and wave loads, and also include a nonlinear interaction with soil at the foundation level. At the same time, the servo-dynamics of the rotor makes the overall assessment and modelling more complicated. Therefore, there is a need for an integrated model which can combine the effects of these parameters. This section introduces a modelling approach for the OWT in the presence of scour and subjected to various loads, which uses OpenFAST and SESAM software. The integrated model can simulate the dynamic responses of the structure (e.g., accelerations) at the tower for different cases.

2.1. OWT Model

In this paper, the NREL 5 MW OWT supported by a monopile foundation is considered as a reference turbine, and is modelled using OpenFAST software. The definition of the NREL 5 MW turbine is described in detail in the report published by Jonkman et al. (2009). Table 1 lists the properties of the turbine. Hub height and rotor diameter are 90 m and 126 m, respectively, where the tower geometry at the bottom is 6 m in diameter and 27 mm in wall thickness. These decrease to 3.87 m and 19 mm at the tower top, respectively. The monopile has a diameter of 6 m with a constant wall thickness of 60 mm above the mudline and 70 mm below the mudline, with a pile embedment length of 51 m in a uniform sand profile. The rated wind speed and rotor speed for the NREL 5 MW system are 11.4 m/s and 12.1 rpm, respectively.

The pile design is provided in Jawalageri et al. (2022), where the pile embedment is designed based on loose sand properties to account for the worst case scenario. This resulted in a 51 m embedment for the pile below the mudline (Arany et al. 2017). OpenFAST currently does not support soil modelling below the mudline, which is a limitation in terms of directly modelling scour erosion. To overcome this challenge, Jawalageri et al. (2022) proposed to use an equivalent spring stiffness at the mudline, which in turn can be incorporated into the OpenFAST model. In this paper, these spring stiffnesses are calculated for each scenario using SESAM software, where the soil profile is modelled by means of sublayers in order to capture the soil interaction with the pile. SESAM characterises the stiffness of the springs at each node of the pile below the mudline for a given load using soil data. SESAM will not consider the soil stiffness for the part of the pile that is affected by scour erosion, i.e. it omits the stiffness contribution lost as a result of scour. For each scour condition and load case, the spring stiffnesses are obtained from SESAM and then imposed at the mudline in the OpenFAST model. In this paper, the soil is modelled assuming medium dense sand with a unit weight of 19 kN/m^3, angle of internal friction of 35 degrees, and initial modulus of subgrade reaction of 2200 kN/m^3 (API 2014). Figure 1 shows the schematic of the OWT system.

Table 1: NREL 5 MW OWT properties (Jonkman et al. 2009)

Description	Value
Rating	5 MW
Configuration	3 blades
Rotor, hub diameter	126 m, 3 m
Hub height	90 m
Rated rotor speed	12.1 rpm
Rotor mass	110,000 kg
Nacelle mass	240,000 kg
Tower mass	347,500 kg
MP Diameter	6.0 m
MP wall thicknesses	0.060 m (above mudline), 0.070 m (below mudline)
Tower top diameter, wall thickness	3.87 m, 0.019 m
Tower base diameter, wall thickness	6.0 m, 0.027 m
Support structure steel density	8500 kg/m^3
Steel Young's modulus	210 GPa
Steel Shear modulus	80.8 GPa

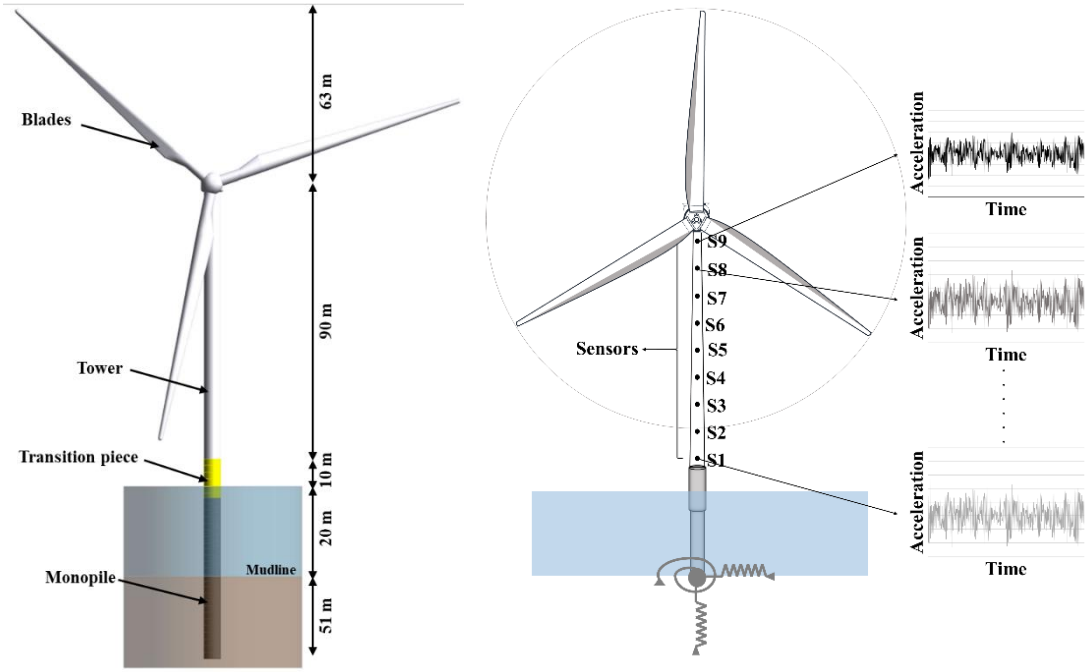

(a) (b)

Figure 1: (a) Schematic of NREL 5 MW OWT; (b) Sensor locations in the simulations.

2.2. Load cases

In this paper, four scour cases are considered with local scour depths of 0 m (no scour), 3 m, 6 m and 9 m. The mudline spring stiffnesses from SESAM were obtained for each scour scenario corresponding to each load case, using the procedure described in section 2.1. The wind speeds as part of the metocean data for the load cases are chosen as values in the vicinity of the rated wind speed of the NREL 5 MW turbine. The surface current velocity of 1.5 m/s is used in this study where the power law is used to calculate the current speed along the depth of the water. The acceleration responses are derived along the tower at nine 'sensor' nodes (see Figure 1b for sensor locations) under different scour conditions. Table 2 summarises the load cases considered.

Table 2: Load case summary

Load Case	Wave height (m)	Wave period (sec)	Uniform wind speed (m/s)
LC1	6	10	10.4
LC2	6	10	10.6
LC3	6	10	10.8
LC4	6	10	11
LC5	6	10	11.2
LC6	6	10	11.4 (Rated wind speed)
LC7	6	10	11.6
LC8	6	10	11.8
LC9	6	10	12
LC10	6	10	12.2

2.3. Acceleration data for training and real-time datasets

The numerical model is used to simulate the acceleration data along the tower for different load cases described in Table 2 for various local scour depths affecting the foundation. A total simulation length of 300 seconds is performed to extract the acceleration data at the nine sensor locations along the tower

(shown in Figure 1b) for each scour case. Table 3 summarizes the number of simulations generated for each scenario for the purpose of generating the training dataset.

Table 3: Labels and total number of tests for each state in offline training mode

Structural State (Class)	Number of simulations
No Scour	10
3 m scour	10
6 m scour	10
9 m scour	10
Total	40

In addition to the training datasets, another dataset is also generated for the real-time mode of the proposed framework. This dataset will be used to evaluate the performance of the ML model on unseen data. These data are generated using three new scour depths corresponding to LC1 and are given in Table 4.

Table 4: Labels and the number of tests for each state to check the accuracy of the framework in real-time mode

Structural State (Class)	Number of simulations
2 m scour	1
4 m scour	1
7 m scour	1

3. Proposed scour detection framework

This study proposes a data-driven structural damage classification methodology that can identify the scour depth affecting an OWT using the acceleration data collected from the tower. The proposed framework consists of three main components, namely, (a) data pre-processing, (b) offline training mode, and (c) real-time classification mode. Figure 2 shows the framework of the proposed algorithm. In the first component, the datasets are pre-processed using a method called data segmentation. This will allow the algorithm to work with shorter-length signals.

In the offline training mode, the feature extraction and feature selection are carried out on the dataset to first extract a set of time domain features, and then to discard features that are not relevant to the classification problem. Further, these selected features are used as inputs to train the supervised machine learning classifier. In the testing and training phase of offline mode, the output of the ML algorithm is a structure state (Class) that is shown in Table 3.

The main problem with this general procedure for testing the trained classifier is that it can be useful for predicting the scour depth around an OWT when the load case of the test dataset is the same as the trained dataset (Najafzadeh et al. (2015), Guan et al. (2022)). This assumption is generally not valid in real cases. Therefore, the result of the trained classifier on real data will be inaccurate. To tackle these challenges, real-time mode has been introduced as the next component after the offline mode. In the real-time monitoring mode, collected data may belong to an assumed load case or it can be from a new load case. The main advantage of the proposed framework is that it can be used for real-time monitoring, where it has a probability distribution for the damage classes, which shows the probability distribution for the percentage of the closeness of the new data to the trained damage classes. Each of these components will be explained in more detail in the following sections.

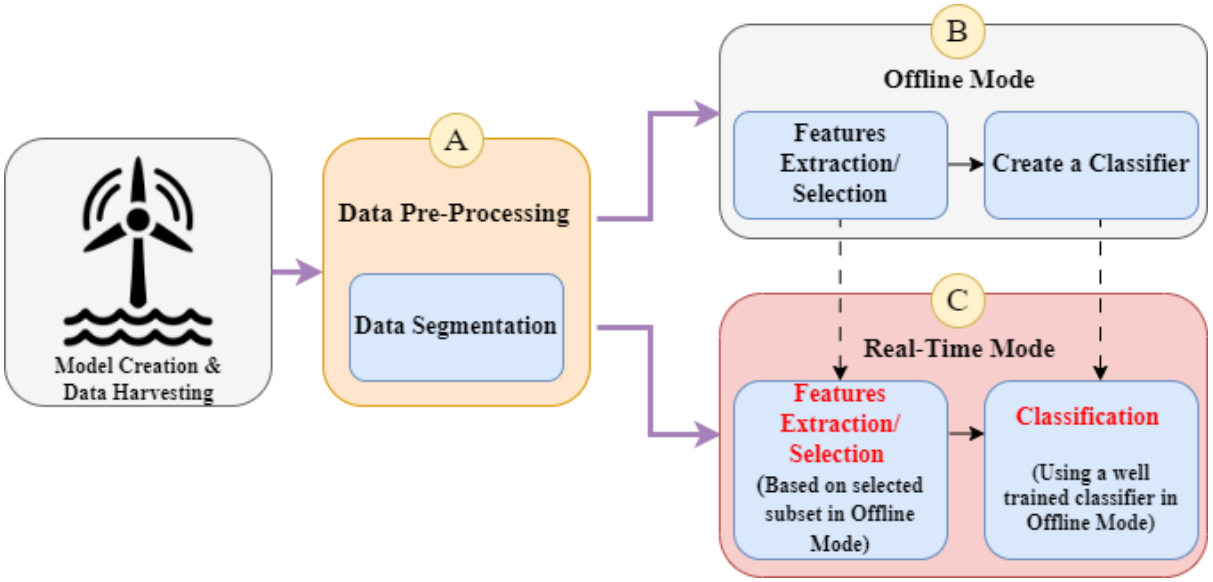

Figure 2: Proposed Framework of scour depth detection for OWTs

3.1. Data segmentation

Figure 3 shows the process of data segmentation on the simulated acceleration response from sensor no. 9 (near the tower top, see Figure 1). The acceleration responses collected from the OWT are segmented using a windowing-based process (Buckley et al. 2022). In this study, each simulation is carried out for a duration of 300 s using a sampling frequency of 1000 Hz. This means that 300,000 time instants are simulated for each signal. It should be noted that a lower sampling rate is possible for these structures, the high rate is used there to ensure rich data is acquired. To create the feature extraction window, the acceleration measurement at a given acquisition time is split into separate windows, and each of these windows shows the response of the OWT in specific time intervals. The time interval is set to be 10 s; therefore, 30 windows of acceleration are created for each response of the OWT under a given load case and scour depth. The features extracted from the acceleration signals are calculated over these time windows, which provide a summary of the dynamic characteristics of the structure over that window. If the sampling rate is changed, the number of analysis windows remains constant, but the number of data points within each window will vary accordingly. Regardless of the sampling rate, the statistical features employed in the study can be derived from the acceleration responses, ensuring flexibility and applicability across different sampling rates.

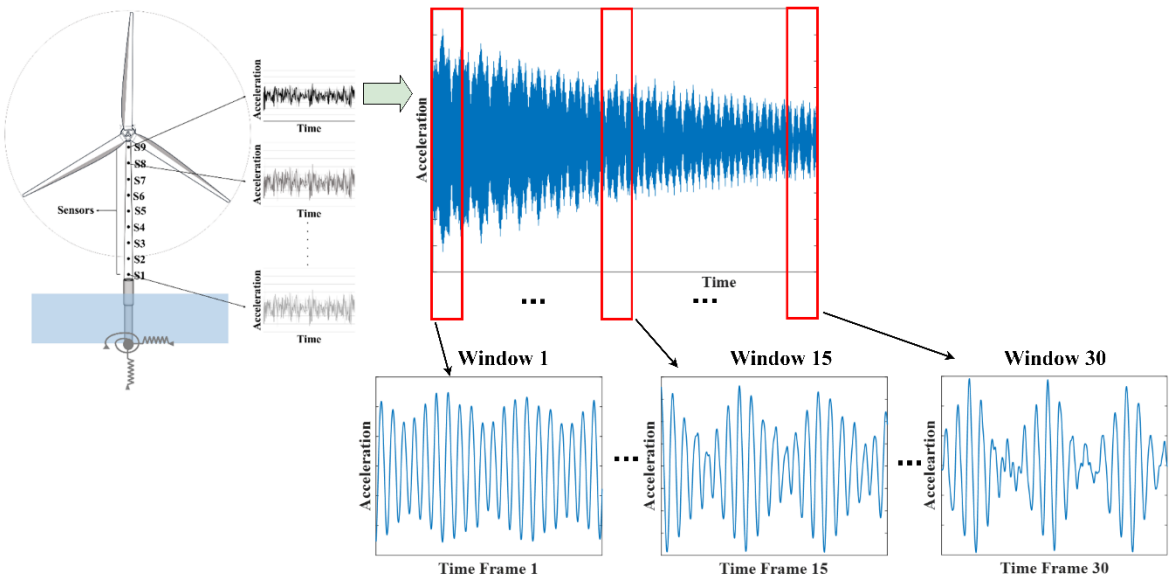

Figure 3: Graphical flowchart of the data segmentation process (Acceleration response for each sensor divided into 30 windows, Total Duration of acceleration signal: 5 min, Duration of each window: 10 s, Sampling Frequency: 1000 Hz)

3.2. Offline mode for training a classifier

The offline classification methodology is derived by first obtaining a training set of data from both scoured and non-scoured structures. Figure 4 shows an overview of the steps involved.

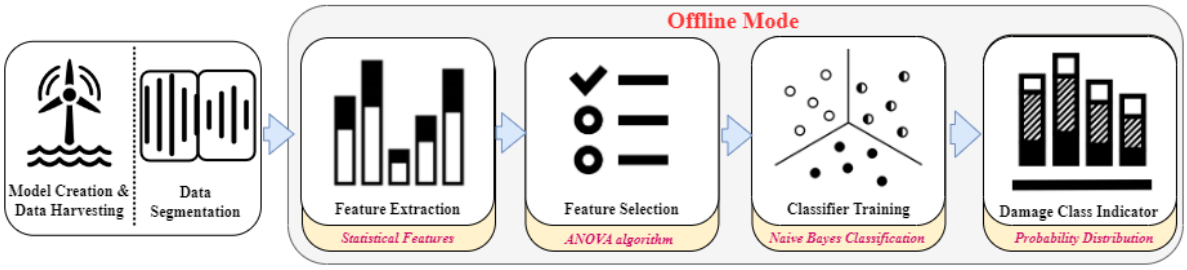

Figure 4: Offline training mode of proposed framework

Statistical features are the simplest features computationally that can be extracted from a signal. These features are computed in the time domain and provide a summary of the statistics of the signal over a time window with a specified length (Ben Ali et al. (2018), Buckley et al. (2022)). The advantage of statistical features is the simplicity of their computation, which becomes particularly important for edge feature extraction on microcontrollers in a wireless sensor network (Ghiasi et al. 2021), for example.

Table 5 gives a summary of the statistical features extracted from the acceleration signals in the present work. These features are selected based on the previous work of authors (Ghiasi et al. 2021) and benchmark studies on feature extraction in SHM (Yang et al. (2007), Ben Ali et al. (2018), Buckley et al. (2022)).

Table 5: Time-domain features

	Feature		Function	Eq.
Statistical Features	Energy of signal	Root mean square	$rms = \sqrt{\frac{\sum_{n=1}^{N}(x(n))^2}{N}}$	(1)
	Time series distribution	Variance	$var = \sigma^2 = \frac{\sum_{n=1}^{N}(x(n) - mean(x))^2}{(N-1)}$	(2)
		Mean	$mean = \frac{1}{N}\sum_{n=1}^{N} x(n)$	(3)
		Skewness	$skewness = \frac{\sum_{n=1}^{N}(x(n) - mean(x))^3}{(N-1)\sigma^3}$	(4)
		Kurtosis	$kurtosis = \frac{\sum_{n=1}^{N}(x(n) - mean(x))^4}{(N-1)\sigma^4}$	(5)
		Shape factor	$sf = \frac{rms}{\frac{1}{N}\sum_{n=1}^{N}\lvert x(n)\rvert}$	(6)
Impulsive Features	Crest factor		$crest = \frac{\max \lvert x(n)\rvert}{rms}$	(7)
	Peak value		$peak = \max \lvert x(n)\rvert$	(8)
	Clearance factor		$cf = \frac{\max \lvert x(n)\rvert}{\left(\frac{1}{N}\sum_{n=1}^{N}\sqrt{\lvert x(n)\rvert}\right)^2}$	(9)
	Impulse factor		$if = \frac{\max \lvert x(n)\rvert}{\frac{1}{N}\sum_{n=1}^{N}\lvert x(n)\rvert}$	(10)
Harmonic Features	Signal to noise and distortion ratio (SINAD)		Ratio of total signal power to total noise-plus-distortion power	
	Total harmonic distortion (THD)		Ratio of total harmonic component power to fundamental power	
	Signal-to-Noise Ratio (SNR)		Ratio of signal power to noise power	

The features shown in Table 5 represent the energy, the time series distribution, and the harmonic and impulsive features of the signal in the time domain (Buckley et al. 2022) and are calculated from the raw acceleration using the above-mentioned equations. When the feature set is extracted, a feature selection method called ANOVA (Kim 2017) is used to reduce the dimension of the problem. In a classification task, a very high-dimensional feature vector, e.g., the features obtained from previous steps, typically leads to the curse of dimensionality problem (Koziel and Leifsson 2013). Moreover, using such features for training classifiers may be a time-consuming procedure. To overcome this, a feature ranking algorithm based on ANOVA is used in this paper. ANOVA is a collection of statistical models that can be used to compare whether two sample's means are significantly different or not. ANOVA tests the null hypothesis, which states that samples in all groups are drawn from populations with the same mean values. To do this, ANOVA compares the distribution variation between groups to the variation within the groups, and provides an F-statistic (Greenland et al. 2016). If the p-value for the F-statistic is smaller than the significance level, then the test rejects the null hypothesis that all class means are equal, and concludes that at least one of the class means is different from the others (Greenland et al. 2016), which in this paper means that the mean of selected feature values differ

between damage classes. The most common significance levels are 0.05 and 0.01. The values of Importance Scores (IS) that are used in this paper as an index for selecting the best features are the negative logs of the p-values.

ANOVA test and rank the features based on their level of variance across the damage states and then a percentage of ANOVA-ranked features are used as the input vector to the damage classification algorithm. By using this method, redundant or highly correlated features are removed.

3.3. Damage detection and classification procedure using Naive Bayes Classifier (NBC)

Bayesian Classification is a process that estimates the probability of a new observation belonging to a predefined category, using a probability model defined according to the theory of Bayes (Cheeseman and Stutz 1996). The technique assesses the prior probability of each category based on a large set of training data, that are described by a number of variables, and assumes that classification could be estimated by calculating the conditional probability density function and the posteriori probability (Soria et al. 2011). The posteriori probability could be calculated according to the equation:

$$p(C_j|X) = \frac{p(X|C_j) \times p(C_j)}{p(X)} \tag{11}$$

where $p(C_j|X)$ is the probability that the unknown observation X belongs to category C_j and is called posteriori probability, $p(X|C_j)$ is the probability, given category C_j, an unknown observation belongs to this category, $p(C_j)$ is the prior probability the unknown observation X to be observed is in category C_j, and $p(X)$ is the prior probability that the unknown observation X is the same for each category C_j.

In the case where all the variables that describe the training data are independent and each of them contributes equally to the problem of classification, a simple method for Bayesian classification known as Naive Bayes has been developed (Soria et al. 2011). The algorithm tends to work well even when the independence assumption is not valid. In addition to the good classification power of the NBC method, the final classifier provides two relevant additional advantages. The first advantage is that for a given sample, the NBC not only provides a prediction for the class of the sample, but also provides a probability of the sample belonging to each class category. This additional information can be used to assess the reliability of the prediction (i.e. it is a very reliable prediction when values of p are close to 1) and to show the behaviour of the classifier when discriminating between classes (for values of p not close to 1, the probabilities associated with each class serve as additional information on possible alternative class predictions). This probability (p) is used as an index in this paper that shows the percentage of the closeness of the new data to the trained scour damage classes.

3.4. k-Fold cross-validation and unbalanced classification performance measures

Before using the classification algorithm to classify new data, it is important to evaluate the performance of the classification algorithm in the offline mode. k-fold cross-validation is one of the most used techniques to determine the training and test datasets when a limited amount of data is available (Leon-Medina et al. 2021). This avoids overfitting and results in a less biased or less optimistic estimate of the model accuracy compared to a simple train/test split. In this study, a 5-fold cross-validation is used to evaluate the performance of the algorithm in the offline mode.

In multiclass classification problems such as the different scour depths considered in this study, each sample from the test dataset has a class label as shown in Table 3 that is compared to the predicted class label. A measure of correctly or incorrectly recognized classes can be defined using a common

index such as precision (specificity), recall (sensitivity), F1-score, etc (Hamidian et al. (2022), Buckley et al. (2022)). On the other hand, to assess the capability of the model for detecting the scour depth affecting an OWT in the real-time mode for unseen data, the traditional performance indices cannot be effective because the output of the model will not be the same as the true class label. Therefore, specific performance measures used in the present work are described as follows:

$$\text{If Predicted class} = \text{True class} \pm 2\text{m} \xrightarrow{yields} \text{True Prediction}$$

$$\text{If Predicted class} > \text{True class} \pm 2\text{m or Predicted class} < \text{True class} \pm 2\text{m} \xrightarrow{yields} \text{False Prediction}$$

This means that if the predicted scour depth is within ±2 m of the actual depth, the prediction will be labelled true, and if it is outside this range, the prediction will be labelled false. Based on the above descriptions the classification accuracy (CA) index can be formulated as below:

$$\text{CA} = \frac{\text{Number of true predictions}}{\text{Total number of predictions}} \tag{12}$$

3.5. Real-time mode for scour detection

Sections 3.2, 3.3 and 3.4 describe the training and validation of NBC using the samples obtained from the FE model of the OWT under different load cases and different scour depths. However, the described strategy is intended to be used for real-time damage detection, which is described herein. Given a new sample associated with an unseen load case or scour depth affecting an OWT, a quick real-time prediction of the scour depth of the structure can be performed. In this context, as stated before, a two-mode strategy is adopted. In the offline stage, the baseline data (set of initial samples based on Table 3 used to generate the NBC) is used to determine the pretrained NBC. The offline stage stores the segmentation process, feature extraction and feature subset selection procedure, and the classifier. This information is then used in the real-time stage for online classification of a new observation. A flowchart of the proposed approach for the real-time mode is depicted in Figure 5, and illustrates the application of the SHM strategy for the new datasets.

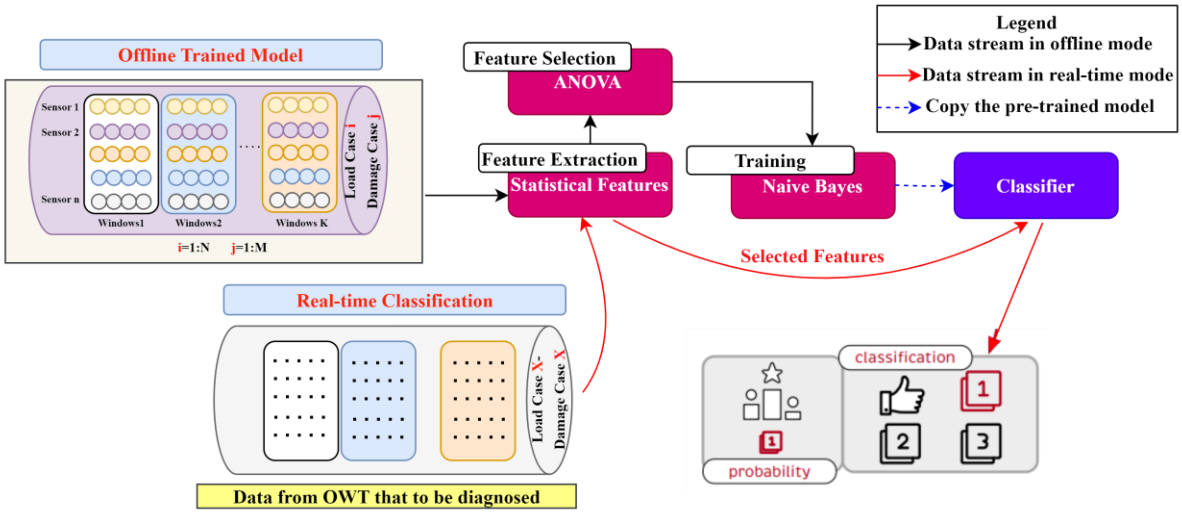

Figure 5: Flowchart of the proposed framework for real-time structural damage diagnosis to classify a new status of an OWT. In this flowchart, *i*=1:N is number of load cases in the offline training mode, and *j*=1:M is the number of damage cases in the offline training mode

As shown in Figure 5, selected features associated with acceleration response of the OWT are directly inserted into the NBC classifier, which returns a set of probabilities $\{p_i\}_{i=1,\dots,l}$ where l denotes the total

number of different structural states and p_i denotes the probability that the sample belongs to the structural state i. Thus, the real-time classification strategy provides the following: (1) the structural state/class prediction; (2) the related probability of class membership p_{max} used for reliability (we can associate a higher or lower level of confidence in our decision based on the value of p_{max}); and (3) probability associated with each of the other structural states.

4. Numerical results

In this section, the numerical data simulated in Section 2 is employed to test the framework proposed in Section 3.

4.1. Feature extraction and feature selection

The acceleration signals simulated in section 2 are extracted at nine points along the tower of the OWT (each representing an accelerometer sensor, see Figure 1). In the feature extraction phase, from each of these acceleration responses, thirteen statistical features are computed based on the equations in Table 5. Therefore, a total of 117 features for each scour depth scenario are considered. These features can be represented against each other. For example, Figure 6a and Figure 6b show the scatter plot of the shape factor of sensor 7 and peak value of sensor 1 grouped by scour depth, and standard deviation (Std) of sensor 3 and skewness of sensor 5 grouped by scour depth, respectively. The scatter plots are normally created to visualize the distributions of various features and it's useful to determine the features that have strong differentiators between various classes of scour.

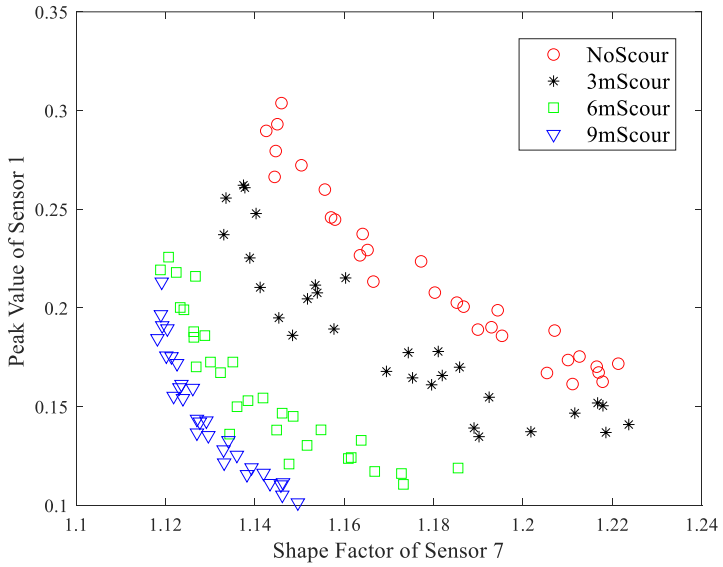

(a)

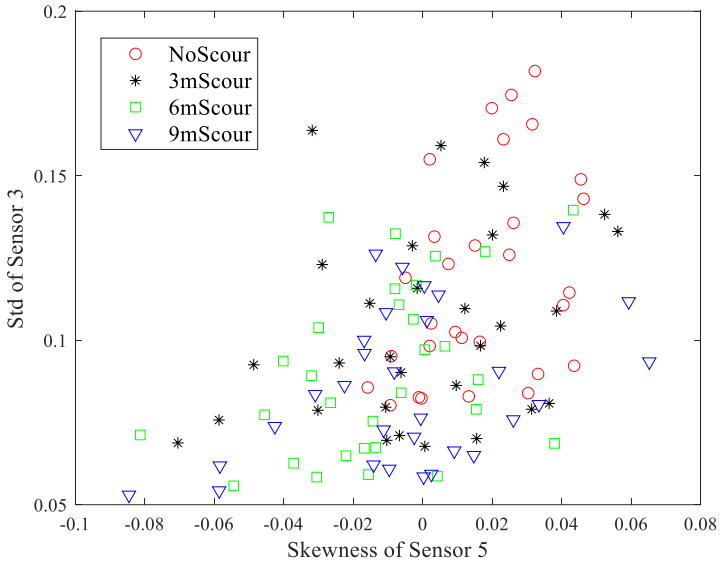

(b)

Figure 6: (a) Scatter plot of shape factor of sensor 7 and peak value of sensor 1 grouped by scour depth; (b) Scatter plot of Std of sensor 3 and skewness of sensor 5 grouped by scour depth

It can be seen in Figure 6a and Figure 6b that some features (such as the peak value of sensor 1 and the shape factor of sensor 7) are showing distinct changes when the depth of scour changes. This indicates that these features can be used in the classification algorithm to detect the depth of scour around the OWT. However, some features such as the standard deviation (std) of sensor 3 or the skewness of sensor 5 could not be completely separated by their scatter plot (classes overlap), suggesting it is not a good fit for the selected subset of features. Although the scatter plot provides an initial understanding of the best features in the SHM system, validating these features using multiple sensors may require multiple visual inputs that can be time consuming. To make this process efficient and objective, the automated ranking method based on the ANOVA algorithm as explained above, is employed. This ranking method calculates and discovers the best features for damage classification in the context of this study. Furthermore, the Kruskal-Wallis is a rank-based non-parametric test that can be used to determine if there are statistically significant differences between two or more groups of an independent variable on a continuous or ordinal dependent variable. It is considered the non-parametric alternative to the one-way ANOVA algorithm (Semwal et al. 2016). Table 6 shows selected features using both ANOVA and Kruskal-Wallis ranking methods.

Table 6: Feature subset selection based on importance using two methods

Selected Features	One way ANOVA IS	Kruskal-Wallis IS
Sensor 7-Shape Factor	34.73	62.03
Sensor 7-Kurtosis	33.92	59.02
Sensor 1-Skewness	33.32	54.19
Sensor 9-Skewness	25.32	45.33
Sensor 1-Peak value	20.59	40.30
Sensor 7-Clearance factor	20.36	42.78
Sensor 3-Peak value	20.35	39.51
Sensor 7-Impulse factor	18.58	40.70
Sensor 7-Crest factor	15.58	34.30
Sensor 9-Kurtosis	15.57	32.28

As can be seen in Table 6, the ANOVA algorithm selects ten features that have minimum intraclass distances and maximum distances between damage classes using IS. These ten features have the largest IS that show they can be used to distinguish different classes of scour.

4.2. Naive Bayes Classifier

Selected features of the previous step are used for the training and testing phase of NBC. The confusion matrices presented in Figure 7 summarize the overall performance of the proposed approach with respect to the actual and predicted classes. An aspect of primary importance for SHM is the separation between healthy and damaged states and the reduction of false alarms. For the no-scour state, 100% of the unseen healthy data is being correctly predicted, and the majority of misclassifications are occurring between successive damage classes with values being misclassified as the previous damage state.

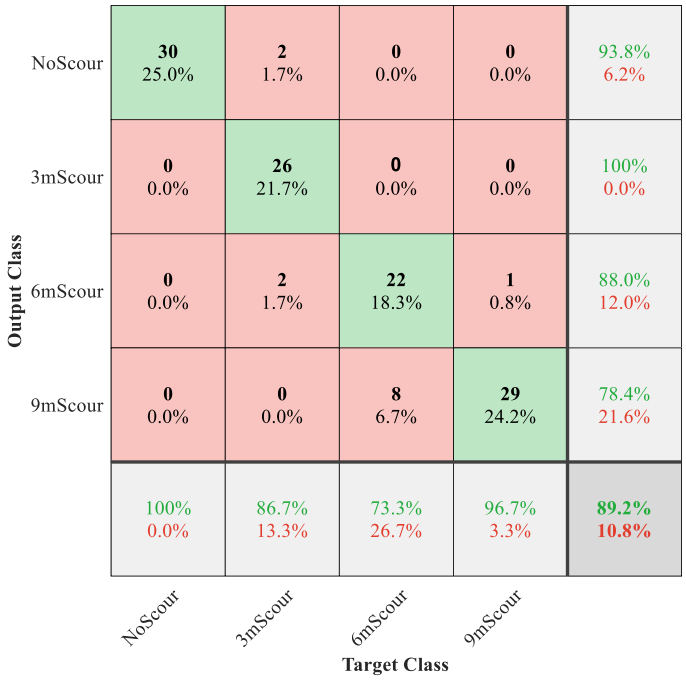

Figure 7: Confusion Matrix for NBC (the result shown based on 5-fold cross-classification accuracy=89.2%)

One of the benefits of the NBC is that it provides a probability-like measure of the sample belonging to this predicted class p_{max} along with the probabilities associated with the other class membership. In the context of scour detection, it means that NBC indicates the probability of new data belonging to each of the pre-trained scour depth classes. Therefore, the reliability of the prediction can be assessed based on these probabilities. As a complement to Figure 7, Figure 8 and Table 7 depict the probability distribution of various scour depth classes for the ten samples.

Table 7: Probability distribution for test data (10% of unobserved data in offline mode)

	Naive Bayes Classifier		Posterior Probability			
	True Labels	**Predicted Labels**	**No-scour**	**3m-Scour**	**6m-Scour**	**9m-Scour**
Test on 10% of unobserved data but in same classes as training data	'3m-Scour'	'3m-Scour'	19.89	80.11	0.00	0.00
	'3m-Scour'	'3m-Scour'	41.14	56.58	2.28	0.00
	'9m-Scour'	'9m-Scour'	0.00	0.12	21.83	78.05
	'6m-Scour'	'6m-Scour'	0.04	18.81	81.15	0.00
	'3m-Scour'	'3m-Scour'	0.65	94.90	4.46	0.00
	'9m-Scour'	'6m-Scour'	0.00	0.03	92.80	7.17
	'3m-Scour'	'3m-Scour'	0.00	100.00	0.00	0.00
	'No-Scour'	'No-Scour'	96.48	3.52	0.00	0.00
	'9m-Scour'	'9m-Scour'	0.00	0.15	30.92	68.93
	'6m-Scour'	'6m-Scour'	0.03	0.52	88.91	10.53

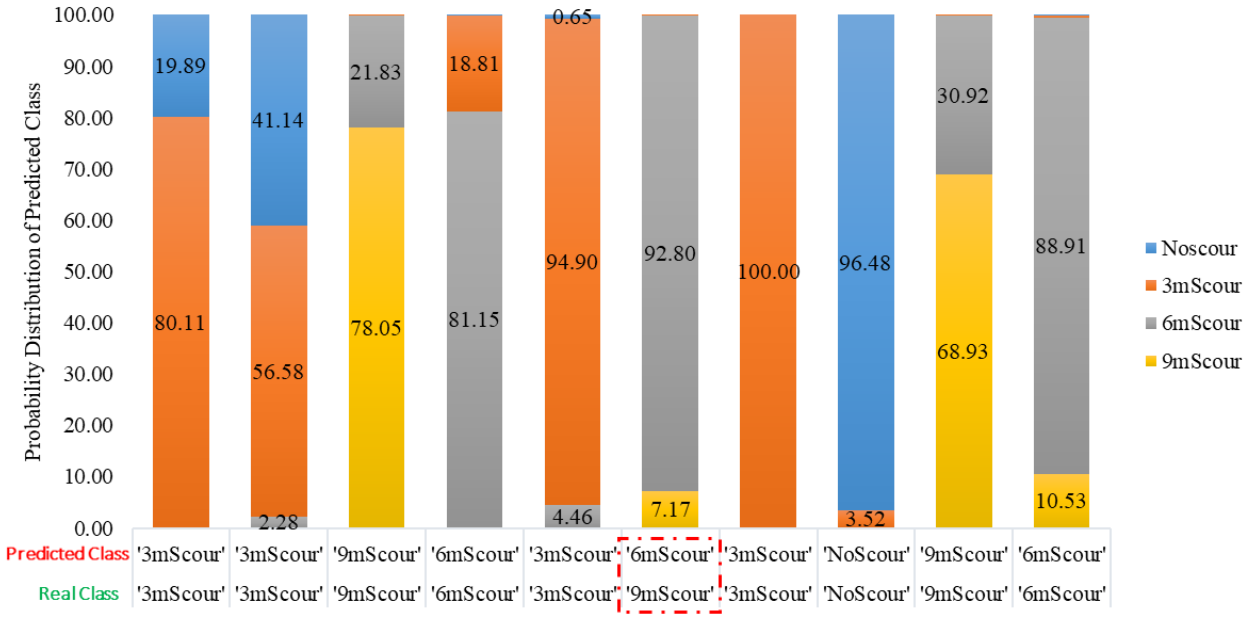

Figure 8: Probability distribution for test data (10% of unobserved data in offline mode). The red box denotes the samples that are incorrectly classified.

In Figure 8, it can be seen that the first two columns are associated with samples where the classifier detects both characteristics of class 1 (no scour) and class 2 (3m scour), even though it correctly detects the predominant class (correct prediction) in all cases. On the other hand, the sample in the sixth column (9 m scour) is wrongly classified as damage class 3 (6 m scour) with a p_{max} = 92%, while the probability associated with the actual class is p_1 = 7.17%. Although the class prediction is incorrect in this case, the actual class is associated with the second maximum probability.

4.3. Comparison with other ML methods in offline mode

To show the robustness of the proposed framework using the NBC algorithm, the same framework is also created by two well-known AI algorithms: SVM (Malekloo et al. 2021) and Artificial Neural Network (ANN) (Avci et al. 2021). The result of using these algorithms as damage classifiers are shown in Figure 9a and Figure 9b, which are based on a 5-fold cross-validation error estimation method. As shown in Figure 9a and Figure 9b, both algorithms had competitive results and the classification accuracy of both are more than 90%. The majority of misclassifications are occurring between successive depth classes with values being misclassified as the previous/next scour depth. The overall accuracy of ANN (93.3%) is slightly better than SVM (92.5%) in this dataset.

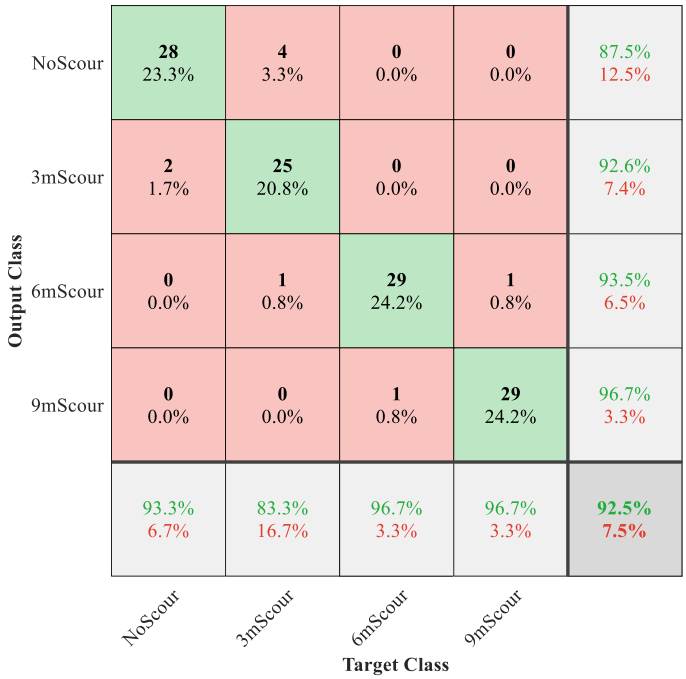

(a)

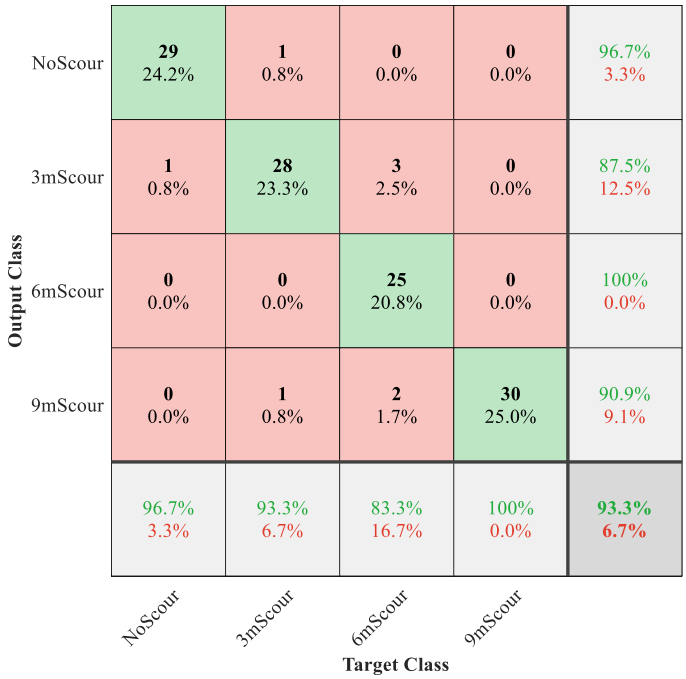

(b)

Figure 9: Training data and validation data are both from same Load Case (a) Confusion Matrix for SVM (Classification Accuracy=92.5%); (b) Confusion Matrix for ANN (Classification Accuracy=93.3%)

4.4. Influence of load case

The influence of different load cases on the accuracy of the proposed framework is demonstrated in Figure 10a and Figure 10b. It is worth noting that for the offline training mode of the algorithm, data

used are from acceleration responses of a structure in LC1 to LC4, and data related to LC5 is not used. Figure 10a and Figure 10b shows the result of SVM and ANN where the testing data are from unseen load case (LC5) but in the same scour depth as the training data.

It can be seen in Figure 10a that the SVM algorithm has good accuracy in detecting scour depth when data comes from 3 m and 6 m classes, but its accuracy comes down when data comes from the 9 m classes or No Scour classes. On the other side, the classification accuracy of ANN (Figure 10b) has better overall accuracy (90.8%) in detecting the true class of scour. From the results presented, it is possible to conclude that the proposed framework has robustness, especially when using the neural network, and its accuracy is acceptable even when the test data comes from untrained load cases that can be applied to the OWT.

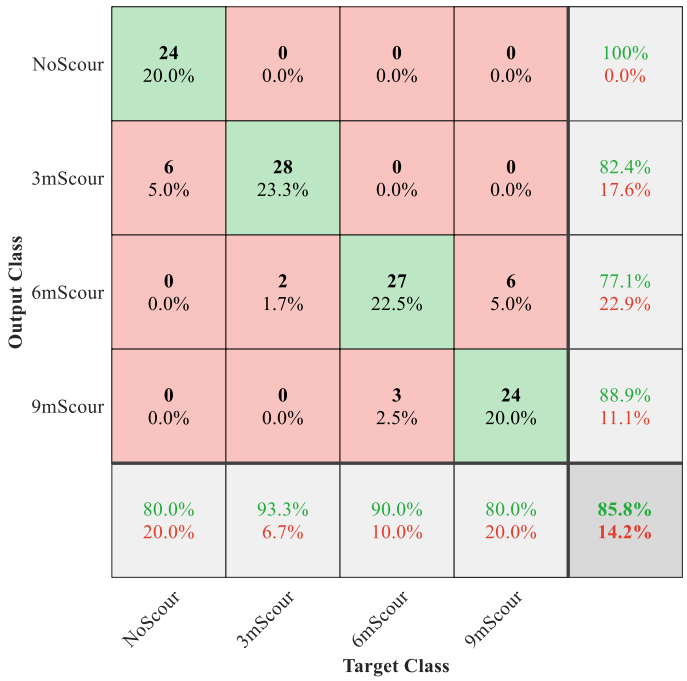

(a)

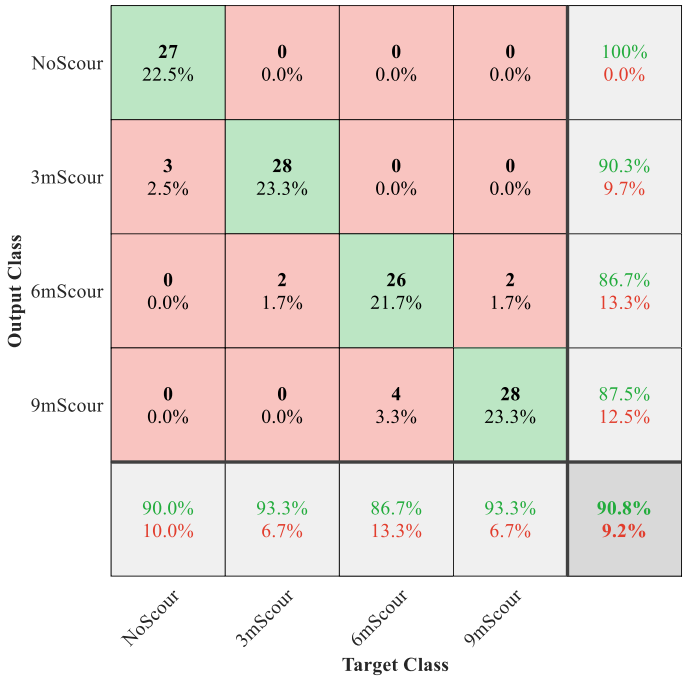

(b)

Figure 10: Training data are from LC1 and Test data are from LC5 (a) Confusion Matrix for SVM; (b) Confusion Matrix for ANN

4.5. Influence of measurement noise

Although simulations cannot fully represent the sources of measurement errors that occur in the real world, a random noise was added to the acceleration signals obtained from OpenFAST to account for measurement errors. In practice, the measured signals may contain errors due to various reasons such as electrical noise, poor installation of sensors, vibrations caused by external sources, among other reasons. The acceleration data obtained from OpenFAST is modified by introducing white noise, which is calculated by using the following equation:

$$a = a_{\text{calc}} + E_P N_{\text{noise}} \sigma(a_{\text{calc}}) \quad (3)$$

where a is the acceleration signal inclusive of noise (polluted acceleration data), a_{calc} is the acceleration data obtained as an output from OpenFAST (noise-free data), E_P is noise level, N_{noise} is a normal distribution with mean value of zero and unit standard distribution, and $\sigma(a_{calc})$ is the standard deviation of noise-free acceleration data. Figure 11a and Figure 11b shows the performance of ANN and SVM models in the presence of noise in the acceleration signals. Both algorithms were trained on noise-free data and tested on data with 3% white noise added to the acceleration response. The overall accuracy of ANN (96.7%) is better than the overall accuracy of SVM (93.3%) for this low noise level. Further, to evaluate the effect of increasing noise level on the accuracy of ANN and SVM models, three higher noise levels of 5%, 8% and 10% are considered and the results are shown in Figure 12. As can be seen in this figure, the accuracy of both models decreases with the increase of the noise level, while the ANN algorithm shows a better overall performance compared to the SVM algorithm. Based on the results, it can be suggested that the proposed framework has an acceptable performance in processing reasonably low noise data.

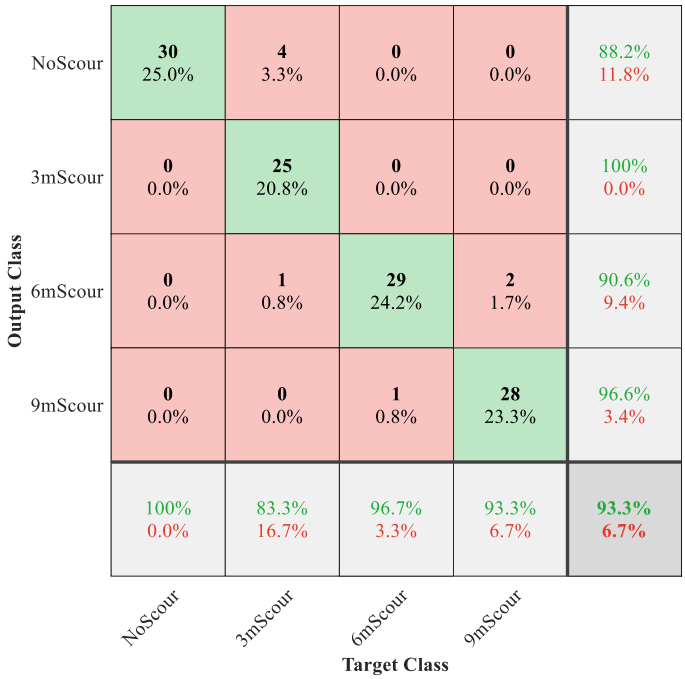

(a)

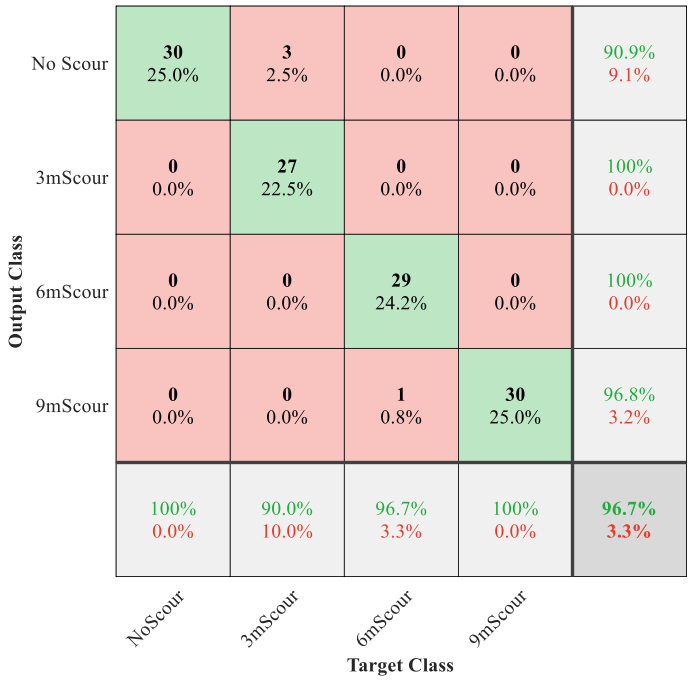

(b)

Figure 11: Training data are from LC1 and Test data are from LC1 with 3% of noise (a) Confusion Matrix for SVM; (b) Confusion Matrix for ANN

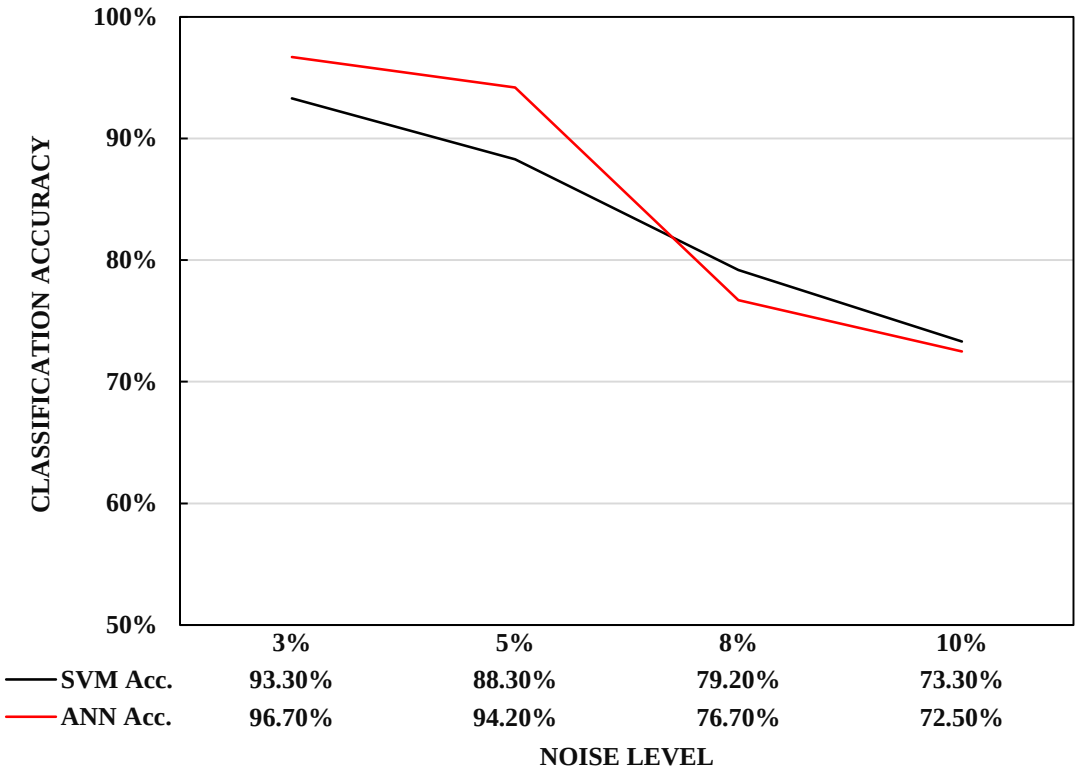

Figure 12: Influence of various noise levels on the accuracy of the SVM and ANN method

4.6. Influence of sensor layout on detection accuracy of the model

The automatic scour depth identification procedure that was applied in the previous sections is based on the responses obtained from five measurement positions (odd numbered sensors in Figure 1). To evaluate whether the number and position of sensors used to detect and classify scour depth can be optimized, the influence of sensor layout is investigated. The main purpose of this analysis is to optimize the number and position of sensors installed along the tower, which reduces the cost of installation and maintenance of sensors, as well as maintains the effectiveness of the defect identification method. In regard to sensor layout, three configurations have been considered which is shown in Table 8. Table 8 also shows the selected feature set and classification accuracy for each layout using SVM and ANN.

Table 8: Sensitivity analysis on the impact of sensor layout on the accuracy of the proposed framework

Selected sensor	Selected feature set by the ANOVA	Classification accuracy using SVM	Classification accuracy using ANN
Odd sensors (S1,S3,S5,S7,S9)	S1-Peak value, S1-Skewness, S3-Peak value-, S7-Clearance factor, S7-Crest factor, S7-Impulse factor, S7-Kurtosis, S7-Shape factor, S9-Kurtosis, S9-Skewness	94.1%	91.6%
Even sensors (S2,S4,S6,S8)	S2-Peak value, S2-Skewness, S4-Peak value, S4-THD, S6-Kurtosis, S6-Shape factor, S8-Clearance factor, S8-Kurtosis, S8-Shape factor, S8-Skewness	91.7%	91.7%

All Sensors	S1-Skewness, S2-Peak value, S3-Skewness, S6-Kurtosis, S6-Shape factor, S7-Kurtosis, S7-Shape factor, S8-Kurtosis, S8-Shape factor, S9-Skewness	96.7%	93.3%

As can be seen in Table 8, the classification accuracies are over 90% for all models. From an economic point of view, with five sensors, it seems possible to accurately classify the scour depth. Moreover, as shown in Jawalageri et al. (2022), for detecting the mode shape of the OWT tower, the best sensor position is to place a sensor at the top and bottom of the tower, which means that the odd sensor layout that considers the first and ninth sensor will achieve a better representation of the status of the OWT.

4.7. Real-time classification

The result of the implementation of the proposed framework on the unseen dataset shown in Table 4 is considered in this section. Figure 13 depicts the predicted class for all 90 samples that are extracted from the scour scenarios in Table 4. The misclassified samples (2, 3, 32, and 90, respectively) are highlighted in red. A high level of confidence is assigned to most classification results (only 4 samples are misclassified) and the accuracy of the model is equal to 95.56%, providing reasonable results.

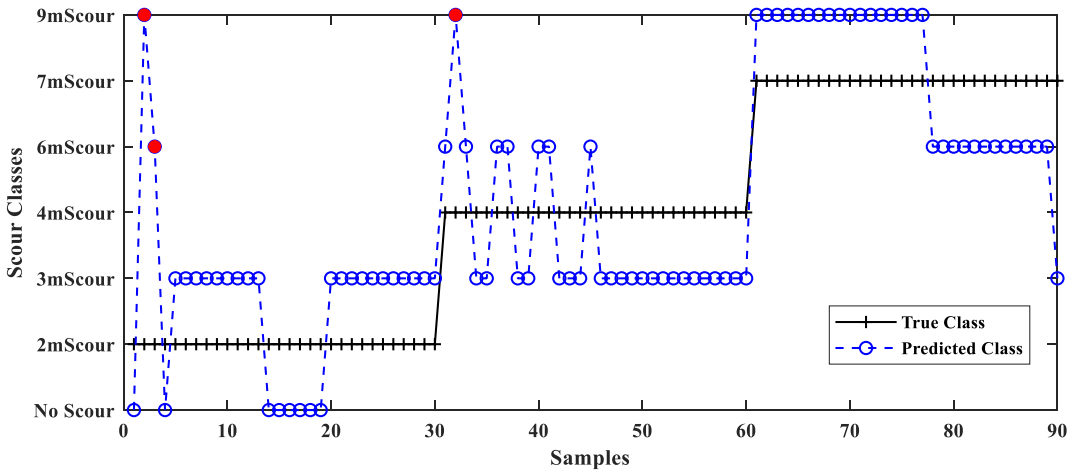

Figure 13: Performance of NBC for unseen data

For samples in which a clear classification is not obtained, the probability distribution provides a better insight into the type of structural state associated with the sample. To show these results, Table 9 and Figure 14 present the probability associated with the predicted classes (scour depth) of ten samples. As can be seen, usually two classes are indicated by the classifier as possible predictions. For example, the first sample comes from 7 m scour depth; but since such a class did not exist in the training mode of the framework, NBC predicts that by a probability of 72% the data comes from a 6 m scour condition, and by a probability of 29% it comes from the scenario that has 9 m scour. As mentioned before the main benefit of the proposed framework is that it can give a likely range for the potential depth of scour around an OWT.

Table 9: Probability distribution for real time mode (new scour depths on which Naive Bayes is not trained)

	Naive Bayes Classifier		Posterior Probability (%)			
	True Labels	Predicted Labels	No-scour	3m-Scour	6m-Scour	9m-Scour
Test on new data set (2 m Scour-	'7m-Scour'	'6m-Scour'	0.00	0.11	71.79	28.10
	'2m-Scour'	'3m-Scour'	0.01	99.99	0.00	0.00
	'2m-Scour'	'3m-Scour'	31.72	68.28	0.00	0.00
	'2m-Scour'	'9m-Scour'	2.66	8.88	43.21	45.25

Naive Bayes Classifier		Posterior Probability (%)			
True Labels	Predicted Labels	No-scour	3m-Scour	6m-Scour	9m-Scour
'2m-Scour'	'No-Scour'	77.48	22.52	0.00	0.00
'7m-Scour'	'9m-Scour'	0.00	0.01	2.41	97.58
'7m-Scour'	'9m-Scour'	0.00	0.03	14.05	85.92
'2m-Scour'	'No-Scour'	70.87	29.13	0.00	0.00
'4m-Scour'	'3m-Scour'	0.01	70.82	22.32	6.84
'7m-Scour'	'9m-Scour'	0.02	0.09	9.60	90.29

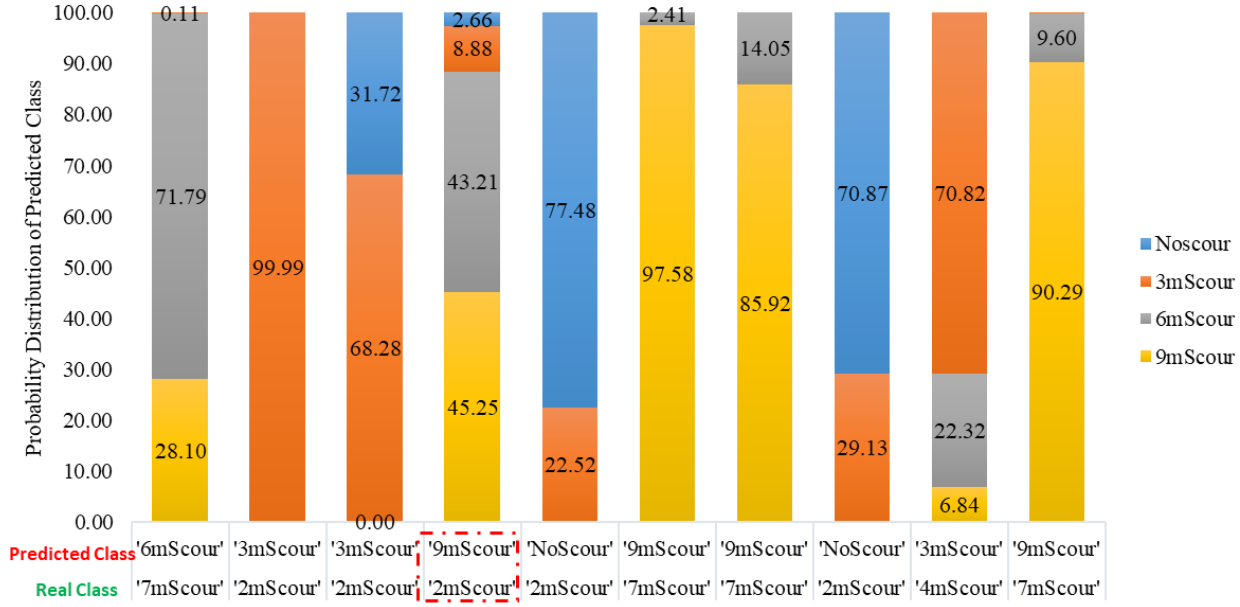

Figure 14: Probability distribution for real-time mode (new scour depths on which Naive Bayes is not trained). The red box denotes the samples that are incorrectly classified.

Based on Figure 14 and Table 9, it can be concluded that the proposed algorithm determines the upper and lower limits of scour depth with very good accuracy when the data is collected in real-time.

4.8. Comparison with other ML methods in real time mode

The performance of ANN and SVM in the case of using new data (ten samples) in the real state are shown in Table 10. As can be seen, both algorithms have an acceptable performance, but the main advantage of NBC's algorithm is that it gives the probability of belonging to pre-trained data classes for unseen data, which makes it possible to determine the upper and lower limits of likely scour depth if the exact class of scour cannot be found.

Table 10: Classification result for real-time mode (new scour depths on which ML is not trained)

Real Scour	SVM output	ANN output
'4m-Scour'	'3m-Scour'	'3m-Scour'
'4m-Scour'	'3m-Scour'	'3m-Scour'
'2m-Scour'	'3m-Scour'	'No-Scour'
'2m-Scour'	'3m-Scour'	'3m-Scour'
'4m-Scour'	'3m-Scour'	'3m-Scour'
'7m-Scour'	'6mS-cour'	'6m-Scour'
'2m-Scour'	'3m-Scour'	'3m-Scour'

'7m-Scour'	'6m-Scour'	'6m-Scour'
'2m-Scour'	'3m-Scour'	'3m-Scour'
'7m-Scour'	'6m-Scour'	'6m-Scour'

5. Conclusion

A vibration-based damage detection and classification methodology was proposed for scour detection of a monopile-supported 5 MW offshore wind turbine in this paper. The approach was tested on a numerical model with four different structural states: an undamaged structure, and a structure affected by 3 m, 6 m, and 9 m of local scour. The developed SHM methodology that combines data pre-processing, feature extraction/selection, and a machine learning classification stage through NBC exhibits a remarkable performance, especially when new unseen data is fed to the framework. The estimation of class membership probabilities using NBC allows the assignment of a high level of confidence to most results. For samples in which a clear classification of scour depth is not obtained, the probability distribution provides a better insight into the type of structure state associated with the sample. In the real-time mode of the proposed framework, NBC predicts the scour depth range of new data by showing the probability distribution for the percentage of closeness of the new data to the trained damage classes. The main conclusions of this work are:

- Feature selection stage is applied to reduce the data volume obtained with the sensors using ANOVA. The results show that by selecting only 10% of features from the feature set, an acceptable accuracy in scour detection can be achieved. These ten features had the largest IS that show they can be used to distinguish different classes of scour.
- The application of the proposed framework was investigated in identifying scour depth in both offline and online modes. In addition, the effect of the change of the applied load, as well as the change in the noise level, was investigated. The results showed that ANN and SVM algorithms have acceptable accuracy in identifying scour depth in these situations.
- The proposed methodology can process new data using the NBC for real-time classification of a new observation. The NBC manages to classify nearly all samples appropriately (only four out of 90 samples are misclassified in the real time mode considered).

Larger OWT structures attract higher aerodynamic and hydrodynamic loads. These increased loads require larger supporting monopile foundations. One consequence of larger diameter monopiles could be the development of larger scour depths around the foundation, as this typically scales with diameter. In light of these emerging challenges, the proposed method outlined in the study has the potential to be a valuable tool for early detection and monitoring of scour that could affect the structural integrity of these emerging OWT foundations.

Future work is expected to focus on two main areas; the possibility of combining both linear and nonlinear feature extraction techniques will be studied to increase the separability capacity of the feature stage before entering the classifier. Furthermore, the developed damage classification methodology will be tested on more complex and realistic structures. It should be noted that the wind speeds considered in this study are around the rated wind speed of the turbine. While the effect of unsteady wind condition such as turbulence along with stochastic waves and currents on the proposed framework has not been studied, this might be a limitation of the proposed method and will be considered as part of future studies. In addition, the validation of the proposed method using real OWT data will be considered as part of the future work.

Acknowledgements

The authors wish to express their gratitude for the financial support received from the Irish Research Council (IRC) EBPPG/2020/259. This publication has also emanated from research conducted with the financial support of Science Foundation Ireland under Grant number 20/FFP-P/8706. The authors are

grateful to Dr Jason Jonkman from National Renewable Energy Laboratory (NREL) for his support with OpenFAST software.

References

Achmus, M., Kuo, Y.-S., Abdel-Rahman, K., 2010. Numerical Investigation of Scour Effect on Lateral Resistance of Windfarm Monopiles, The Twentieth International Offshore and Polar Engineering Conference, International Society of Offshore and Polar Engineers, Beijing, China.

API, 2014. Geotechnical and Foundation Design Considerations.

Arany, L., Bhattacharya, S., Macdonald, J., Hogan, S.J., 2017. Design of monopiles for offshore wind turbines in 10 steps. Soil Dynamics and Earthquake Engineering 92, 126-152.

Avci, O., Abdeljaber, O., Kiranyaz, S., Hussein, M., Gabbouj, M., Inman, D.J., 2021. A review of vibration-based damage detection in civil structures: From traditional methods to Machine Learning and Deep Learning applications. Mechanical Systems and Signal Processing 147.

Ben Ali, J., Saidi, L., Harrath, S., Bechhoefer, E., Benbouzid, M., 2018. Online automatic diagnosis of wind turbine bearings progressive degradations under real experimental conditions based on unsupervised machine learning. Applied Acoustics 132, 167-181.

Bennett, C.R., Lin, C., Parsons, R., Han, J., 2009. Evaluation of Behavior of a Laterally Loaded Bridge Pile Group under Scour Conditions, Structures Congress 2009, pp. 1-10.

Biogradlija, A., 2022. Siemens Gamesa debuts 14 MW turbine at Moray West in UK.

Buckley, T., Ghosh, B., Pakrashi, V., 2022. A Feature Extraction & Selection Benchmark for Structural Health Monitoring. Structural Health Monitoring.

Cheeseman, P.C., Stutz, J., 1996. Bayesian Classification AutoClass: Theory and Results. Advances in knowledge discovery and data mining.

Civera, M., Surace, C., 2022. Non-Destructive Techniques for the Condition and Structural Health Monitoring of Wind Turbines: A Literature Review of the Last 20 Years. Sensors (Basel) 22 (4).

Devriendt, C., Magalhães, F., Weijtjens, W., De Sitter, G., Cunha, Á., Guillaume, P., 2014. Structural health monitoring of offshore wind turbines using automated operational modal analysis. Structural Health Monitoring 13 (6), 644-659.

DNVGL, 2016. DNV-ST-0126 Support structures for wind turbines.

Duguid, L., 2017. OFFSHORE WIND FARM SUBSTRUCTURE MONITORING AND INSPECTION Catapult Offshore Renewable Energy.

Ghiasi, R., Ghasemi, M.R., Chan, T., 2021. Optimum feature selection for SHM of benchmark structures using efficient AI mechanism, in: 27, S.S.S. (Ed.).

Greenland, S., Senn, S.J., Rothman, K.J., Carlin, J.B., Poole, C., Goodman, S.N., Altman, D.G., 2016. Statistical tests, P values, confidence intervals, and power: a guide to misinterpretations. Eur J Epidemiol 31 (4), 337-350.

Guan, D.-w., Xie, Y.-x., Yao, Z.-s., Chiew, Y.-M., Zhang, J.-s., Zheng, J.-h., 2022. Local scour at offshore windfarm monopile foundations: A review. Water Science and Engineering 15 (1), 29-39.

Hamidian, P., Soofi, Y.J., Bitaraf, M., 2022. A comparative machine learning approach for entropy-based damage detection using output-only correlation signal. Journal of Civil Structural Health Monitoring 12 (5), 975-990.

Jawalageri, S., Prendergast, L.J., Jalilvand, S., Malekjafarian, A., 2022. Effect of scour erosion on mode shapes of a 5 MW monopile-supported offshore wind turbine. Ocean Engineering 266.

Jeong, S., Kim, E.-J., Shin, D.H., Park, J.-W., Sim, S.-H., 2020. Data fusion-based damage identification for a monopile offshore wind turbine structure using wireless smart sensors. Ocean Engineering 195.

Jonkman, J., Butterfield, S., Musial, W., Scott, G., 2009. Definition of a 5-MW Reference Wind Turbine for Offshore System Development. National Renewable Energy Laboratory.

Kim, T.K., 2017. Understanding one-way ANOVA using conceptual figures. Korean J Anesthesiol 70 (1), 22-26.
Kolios, A., Smolka, U., Ramdane, C.B., Tremps, L., Jones, R., 2018. Monitoring technology and specification of the support structure monitoring problem for offshore wind farms.
Koziel, S., Leifsson, L., 2013. Surrogate-based modeling and optimization. Springer.
Leon-Medina, J.X., Anaya, M., Pares, N., Tibaduiza, D.A., Pozo, F., 2021. Structural Damage Classification in a Jacket-Type Wind-Turbine Foundation Using Principal Component Analysis and Extreme Gradient Boosting. Sensors (Basel) 21 (8).
Malekloo, A., Ozer, E., AlHamaydeh, M., Girolami, M., 2021. Machine learning and structural health monitoring overview with emerging technology and high-dimensional data source highlights. Structural Health Monitoring 21 (4), 1906-1955.
Mayall, R.O., Byrne, B.W., Burd, H.J., McAdam, R.A., Cassie, P., Whitehouse, R.J.S., 2018. Modelling of foundation response to scour and scour protection for offshore wind turbine structures.
Michalis, P., Saafi, M., Judd, M., 2013. Capacitive sensors for offshore scour monitoring. Proceedings of the Institution of Civil Engineers - Energy 166 (4), 189-197.
Mousavi, Z., Varahram, S., Ettefagh, M.M., Sadeghi, M.H., Razavi, S.N., 2020. Deep neural networks–based damage detection using vibration signals of finite element model and real intact state: An evaluation via a lab-scale offshore jacket structure. Structural Health Monitoring 20 (1), 379-405.
Najafzadeh, M., Barani, G.-A., Hessami-Kermani, M.-R., 2015. Evaluation of GMDH networks for prediction of local scour depth at bridge abutments in coarse sediments with thinly armored beds. Ocean Engineering 104, 387-396.
Nanda Kishore, Y., Narasimha Rao, S., Mani, J.S., 2009. The behavior of laterally loaded piles subjected to scour in marine environment. KSCE Journal of Civil Engineering 13 (6), 403-408.
Peder Hyldal Sørensen, S., Bo Ibsen, L., 2013. Assessment of foundation design for offshore monopiles unprotected against scour. Ocean Engineering 63, 17-25.
Prendergast, L.J., Gavin, K., Doherty, P., 2015. An investigation into the effect of scour on the natural frequency of an offshore wind turbine. Ocean Engineering 101, 1-11.
Reese, L.C., Wang, S.T., Long, J.H., 1989. Scour From Cyclic Lateral Loading of Piles, All Days.
Sánchez, S., López-Gutiérrez, J.-S., Negro, V., Esteban, M.D., 2019. Foundations in Offshore Wind Farms: Evolution, Characteristics and Range of Use. Analysis of Main Dimensional Parameters in Monopile Foundations. Journal of Marine Science and Engineering 7 (12).
Schröder, K., Gebhardt, C.G., Rolfes, R., 2017. A two-step approach to damage localization at supporting structures of offshore wind turbines. Structural Health Monitoring 17 (5), 1313-1330.
Semwal, V.B., Singha, J., Sharma, P.K., Chauhan, A., Behera, B., 2016. An optimized feature selection technique based on incremental feature analysis for bio-metric gait data classification. Multimedia Tools and Applications 76 (22), 24457-24475.
Shadlou, M., Bhattacharya, S., 2016. Dynamic stiffness of monopiles supporting offshore wind turbine generators. Soil Dynamics and Earthquake Engineering 88, 15-32.
Soria, D., Garibaldi, J.M., Ambrogi, F., Biganzoli, E.M., Ellis, I.O., 2011. A 'non-parametric' version of the naive Bayes classifier. Knowledge-Based Systems 24 (6), 775-784.
Tang, D., Zhao, M., 2021. Real-time monitoring system for scour around monopile foundation of offshore wind turbine. Journal of Civil Structural Health Monitoring 11 (3), 645-660.
Tempel, J.v.d., Zaaijer, J.M.B., Subroto, H., 2004. The effects of scour on the design of offshore wind turbines, Proceedings of the 3rd International Conference on Marine Renewable Energy – MAREC, Blyth, UK, pp. 27–35.
Tian, Z., Liu, F., Zhou, L., Yuan, C., 2020. Fluid-structure interaction analysis of offshore structures based on separation of transferred responses. Ocean Engineering 195.
Wang, X., Zeng, X., Li, J., Yang, X., Wang, H., 2018. A review on recent advancements of substructures for offshore wind turbines. Energy Conversion and Management 158, 103-119.

Weijtjens, W., Verbelen, T., De Sitter, G., Devriendt, C., 2016. Foundation structural health monitoring of an offshore wind turbine—a full-scale case study. Structural Health Monitoring 15 (4), 389-402.
Weinert, J., Smolka, U., Schümann, B., Cheng, P.W., 2015. Detecting critical scour developments at monopile foundations under operating conditions, EWEA 2015 Scientific Proceedings, Paris.
Whitehouse, R.J.S., Harris, J., Sutherland, J., Rees, J., 2008. An assessment of field data for scour at offshore wind turbine foundations, ICSE 2008 (4th International Conference on Scour and Erosion), Tokyo.
WindEurope, 2021. Offshore Wind in Europe, Key trends and statistics 2020.
WindEurope, 2022. Offshore wind energy 2022 mid-year statistics.
Yang, J., Zhang, Y., Zhu, Y., 2007. Intelligent fault diagnosis of rolling element bearing based on SVMs and fractal dimension. Mechanical Systems and Signal Processing 21 (5), 2012-2024.
Zhang, A., Li, M., Zhou, L., 2018. Structural Health Monitoring of Offshore Wind Turbine based on Online Data-driven Support Vector Machine, 2018 IEEE 7th Data Driven Control and Learning Systems Conference (DDCLS), pp. 990-995.